

The phase-delay spectrum of GX 5-1 on its normal branch

B.A. Vaughan^{1,2}, M. van der Klis², W.H.G. Lewin³, J. van Paradijs^{2,4}, K. Mitsuda⁵, and T. Dotani⁵

¹ Space Radiation Laboratory, California Institute of Technology, MC 220-47, Pasadena CA 91125, USA

² Astronomical Institute “Anton Pannekoek”, University of Amsterdam and Center for High Energy Astrophysics, Kruislaan 403, 1098 SJ Amsterdam, The Netherlands

³ Massachusetts Institute of Technology, 37-627, Cambridge, MA 02139, USA

⁴ Physics Department, University of Alabama in Huntsville, Huntsville AL 35899, USA

⁵ Institute of Space and Astronautical Sciences, 3-1-1 Yoshinodai, Sagamihara-shi, Kanagawa-ken, 229 Japan

Received 2 October 1997 / Accepted 6 April 1998

Abstract. We have measured the phase differences between X-ray intensity variations in different energy bands in data taken with *Ginga* of the Z source GX 5-1 in its normal branch. We apply a χ^2 optimal extraction technique to measure the phase-delay spectrum of the normal-branch quasi-periodic oscillations (QPO) and find a jump at 3.5 keV. X-ray intensity variations at the QPO frequency in energy channels below 3.5 keV are in phase with one another. The same is true of energy channels above 6 keV. However, intensity variations in energy channels above 6 keV lag those in channels below 3.5 keV by $\sim 150^\circ$. We see no minimum in the fractional rms amplitude of the quasi-periodic oscillations at the jump energy, in contrast to what is seen in the Z source Cyg X-2, but because of limited statistics we cannot rule out such a minimum. We discuss our findings in the context of a radiation-hydrodynamics model for the normal-branch quasi-periodic oscillations.

Key words: accretion, accretion disks – stars: individual: GX 5-1 – stars: neutron – X-rays: stars

1. Introduction

Studies of fast timing variability, and correlated spectral variability, in luminous X-ray binaries during the past ten years have shown that six of the brightest persistent low-mass X-ray binaries form a class; they are called Z sources (Hasinger & van der Klis 1989). The spectral state of a low-mass X-ray binary is defined using an X-ray color-color diagram whose x-axis is the ratio of count rate at intermediate energies (typically 3-6 keV) to low energies (typically 1-3 keV) and whose y-axis is the ratio of count rate at high energies (typically 6-12 keV) to intermediate energies (typically 3-6 keV). As the spectrum varies in time, the source moves through the diagram, tracing out a characteristic pattern. The position of the source in the diagram defines its spectral state. Z sources derive their name from the fact that the track they trace out in color-color diagrams is approximately Z shaped for several sources. Spectral state varies smoothly but

stochastically, and a typical Z source traces out a Z pattern in a couple of days. The three limbs of the Z are called the horizontal, normal and flaring branches, from upper left to lower right.

Spectral variability, or equivalently motion along the Z pattern, has a time scale of hours to days. The properties of the fast X-ray variability, on a time scale of milliseconds to tens of seconds, are strongly correlated with spectral state. Position in the Z pattern dominates the fast timing properties (Hasinger & van der Klis 1989, Hertz et al. 1992, Lewin et al. 1992). On the horizontal branch, high frequency quasi-periodic oscillations with full widths at half maximum of 5-10 Hz and centroid frequencies of 13-55 Hz that are strongly correlated with intensity, and with position along the Z track, have been observed in 4 of the 6 Z sources. On the normal branch, normal-branch QPO with centroid frequencies of ~ 6 Hz are observed. The combination of relatively high frequency and low fractional root-mean-squared (rms) variability amplitude (typically 0.01-0.1) nearly always make it necessary to study their properties using Fourier techniques.

Spectrally resolved, high count rate, high time resolution X-ray data have made it possible to study the energy dependence of quasi-periodic oscillations. The fractional rms amplitude of QPO is measured by fitting the power spectrum of data containing QPO using a function that includes a broad peak, usually modeled as a Lorentzian, and additional terms to model the other observed noise features. See Lewin, van Paradijs & van der Klis (1988) or van der Klis (1989b) for discussions of low-mass X-ray binary power spectra and fitting. The fractional rms amplitude of both horizontal and normal branch QPO have been found to increase with photon energy in GX 5-1 and Cyg X-2 (van der Klis 1986; Dotani 1988; Mitsuda & Dotani 1989; Lewin et al. 1992). We call fractional rms amplitude as a function of energy the “rms amplitude spectrum”. In addition to rms amplitude spectra, one can use cross spectra to measure phase differences, or equivalently time differences, between quasi-periodic oscillations at different energies. We call time, or phase, differences as a function of energy “time-delay spectra”, or “phase-delay spectra”. Van der Klis et al. (1987) were the first to use cross

Send offprint requests to: M. van der Klis

spectra to investigate time delays between rapid intensity variation in low-mass X-ray binaries. They found that on the horizontal branch, high energy intensity fluctuations at QPO frequencies lagged low energy fluctuations by several milliseconds in Cyg X-2, and saw hints of a similar, but less statistically significant, delay in GX 5-1. Subsequently, Mitsuda & Dotani (1989) discovered time differences of about 70 ms between normal-branch quasi-periodic oscillations at energies below and above about 6 keV in Cyg X-2. At the normal-branch QPO frequency of ~ 6 Hz, a 70 ms time difference corresponds to a phase difference of about 150° . Interestingly, they also found a minimum in the QPO rms amplitude spectrum at 6 keV.

A radiation-hydrodynamics model of normal branch quasi-periodic oscillations has been developed (Lamb 1989; Fortner, Lamb & Miller 1989; Miller & Lamb 1992) that proposes changes in the optical depth of the radial inflow near the neutron star as the source of normal branch oscillations. These optical depth changes produce a “pivoting” of the X-ray spectrum. Intensity variations at energies below the pivot energy should be out of phase with intensity variations at energies above the pivot energy, and there should be a minimum in the rms amplitude spectrum at the pivot energy. The model is consistent with the rms amplitude spectrum and time-delay spectrum observed in data from Cyg X-2 on the normal branch.

GX 5-1 is in many ways Cyg X-2’s smarter brother (brighter twin). We expected that the same rms amplitude spectrum and phase-delay spectrum seen in Cyg X-2 should be present in GX 5-1. We recently developed a symmetric, χ^2 optimal extraction method for determining phase-delay spectra and applied it to data taken during a *Ginga* observation of GX 5-1 on the horizontal branch (Vaughan et al. 1994). We here apply the same method to the normal-branch quasi-periodic oscillations and find that the large phase differences observed on the normal branch in Cyg X-2 are indeed present in GX 5-1, but that the jump in the phase-delay spectrum occurs at a much lower photon energy (3.5 keV, rather than 6 keV). Our data are not of sufficient statistical quality to rule out a minimum in the rms amplitude spectrum as is seen in Cyg X-2.

2. Observations

The Large Area Counter (LAC) on *Ginga* (Makino et al. 1987; Turner et al. 1989) was used to observe GX 5-1 from 1 to 6 September, 1991. Data were taken in MPC-3 mode, with 12 energy spectral channels in the range 1.2-18.4 keV and a time resolution of 1/128 s. For analysis, the data were rebinned into 10 spectral channels. On September 4th, GX 5-1 was on the normal branch, with a count rate in the range 8300-9300 counts per second. Corrected for aspect, background and instrumental deadtime, the estimated incident count rate was 10400-12600 counts per second, approximately one crab. During the remainder of the observation, GX 5-1 was on the horizontal branch (see Lewin et al. 1992, for a detailed analysis of the QPO and noise characteristics using the same data set).

3. Analysis techniques

3.1. Phase and time delay measurements

Traditionally, given two or more energy channels, phase (or time) delays between variations in these channels have been measured by choosing one channel, call it m , as a reference, and computing the cross spectrum, $G_{mn}(\nu)$, between all other channels, n , and the reference channel. The phase difference (in radians) between channels m and n is given by the phase of $G_{mn}(\nu)$. The χ^2 optimum extraction method for computing phase and time-delay spectra, given $N_c > 3$ energy channels, that we use in this paper, is described in detail in Vaughan et al. (1994). Briefly, it involves measuring the cross spectrum, $G_{mn}(\nu)$, between all $N_c(N_c - 1)/2$ pairs of energy channels, averaging over a frequency range of interest to obtain \hat{G}_{mn} , which we call the average cross amplitude, or cross amplitude, and fitting the average cross amplitudes with the model $\hat{G}_{mn} = H_m^* H_n$, where the (complex) fit parameters, H_m , are transfer functions. The underlying assumption (verifiable from the χ^2 value of the best fit) is that the X-ray light curve in each energy channel is related to the others by a linear transformation. We choose to define phase on $[-\frac{1}{2}, \frac{1}{2}]$. Phase differences between variations in channels m and n , in the frequency range of interest, are given by $\delta\phi_{mn} = \frac{1}{2\pi} \arg[H_m^* H_n]$. The time difference at frequency ν is $\delta t_{mn} = \frac{1}{\nu} \delta\phi_{mn}$. A positive phase difference indicates variations in channel n precede those in channel m . The advantages of the χ^2 best fit technique are that it uses all available information, and is symmetric in the sense that all energy channels are treated the same. It is closely analogous to synthesis imaging in radio astronomy.

3.2. Deadtime and cross talk

Each time an X-ray photon is detected, there is a fixed instrumental deadtime during which no additional photons can be detected. In *Ginga*, this deadtime is independent of the readout (binning) cycle of the electronics, and is dominated by the ADC (analog to digital converter). Each of the eight proportional counters on *Ginga* has its own electronics, each with a deadtime per event of $206 \pm 1 \mu\text{s}$, independent of energy (Mitsuda & Dotani 1989).

Deadtime has several consequences. First, the measured total flux and total fractional amplitude of modulation will be smaller than the intrinsic flux and fractional amplitude of modulation. The amplitude of modulation inferred from a feature in a power spectrum hence must be corrected for deadtime. Second, an increase in observed count rate in one energy channel results in increased deadtime and a subsequent suppression of the count rate in all channels, an effect known as “cross talk”. Cross talk introduces an anticorrelation between energy channels, that must be corrected for in rms amplitude spectra and cross spectra. Cross talk has two forms. First, variations in the intrinsic X-ray luminosity in any one energy channel will cause variations in the live time, and thereby induce modulations in the other channels 180° out of phase with the modulations in that channel. Second, statistical (Poisson) fluctuations in one chan-

nel will be anticorrelated with statistical variations in the others, resulting in an anomalously small value of the cross correlation at zero lag, and a negative real part in the cross spectrum that is independent of frequency. See van der Klis et al. (1987, 1989a), Lewin et al. (1988) or Mitsuda & Dotani (1989) for discussions of instrumental deadtime.

Because the phenomenon we are investigating, namely, a nearly 180° phase difference between fluctuations in different energy channels, closely resembles the effect of cross talk, we corrected all rms-amplitude spectra and phase difference measurements with three independent techniques and checked for consistency.

1. Because the cross spectrum induced by statistical fluctuations is independent of frequency, one can estimate it by averaging the observed cross spectrum over frequencies high enough to be unaffected by the source variability. To correct the measured cross spectrum in a frequency range of interest, subtract the “source free” average cross spectrum from the cross spectrum at each Fourier frequency (van der Klis et al. 1987).
2. In the absence of deadtime the number of photons in each time bin in each energy channel is Poisson distributed. Deadtime modifies the distribution and causes the probabilities to be covariant. Consider two energy channels. From the measured average count rates in each channel and the known deadtime per event one can calculate the modified probability distribution, $P(\mu_1, \mu_2)$, of detecting μ_1 photons in channel 1 and μ_2 photons in channel 2 (Mitsuda & Dotani 1989). The covariance between the channels, which will be negative, can be computed numerically from $P(\mu_1, \mu_2)$. From the covariance, it is possible to follow the technique described in van der Klis (1989a) to calculate the cross spectrum induced by statistical fluctuations and subtract it from the measured cross spectrum at all Fourier frequencies.
3. Because we know the number of counts per time bin, we can correct the raw counts by converting them into counts per live time in each time bin in each energy channel before transforming the data. Mitsuda & Dotani (1989) find from Monte-Carlo simulations that this technique removes cross talk induced by luminosity fluctuations. We found that this procedure also removes cross talk induced by statistical fluctuations. This was a surprising result to us that we tested both with Monte Carlo simulations and with real data from a number of sources. We found that using counts per live time removes cross talk induced by statistical fluctuations provided the number of counts per bin is neither too small (a few counts per bin) nor too large (more than about 50% deadtime). Low count rates are not a problem in practice as cross talk is then negligible and requires no correction. For extremely high count rates, cross talk is a real problem, and probably cannot be handled by any of the techniques described here

The first two techniques above remove only the statistical cross talk. After applying these, it is necessary to remove the cross talk induced by luminosity fluctuations (van der Klis

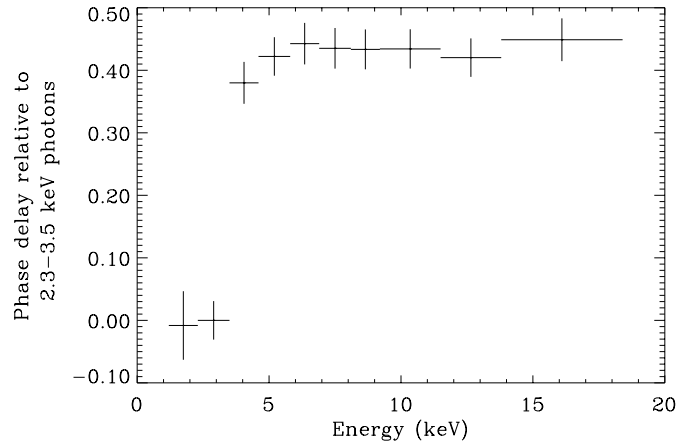


Fig. 1. Phase delay spectrum of GX 5-1, observed in 4-8 Hz on the lower normal branch. Strong 6 Hz normal-branch QPO are present. The phase difference between channels 1-2 and channels 5-10 is $151 \pm 11^\circ$ normal branch.

1989a; Lewin et al. 1988). However, in our case cross talk induced by luminosity fluctuations was small enough to be neglected. It is of course much smaller than cross talk induced by statistical fluctuations, as the total fractional rms amplitude of statistical fluctuations (about 10%-20%) is a factor of 10 larger than the fractional rms amplitude of the QPO.

4. Results

The detailed spectral and correlated timing behavior of GX 5-1 from the 1991 September 4 observation have been reported by Lewin et al. (1992). Normal-branch quasi-periodic oscillations were observed when the source was below the center of the normal branch; the “lower normal branch”. Phase-delay spectra of the GX 5-1 normal-branch oscillations observed on the lower normal branch are shown in Fig. 1. Phase is defined on $[-\frac{1}{2}, \frac{1}{2}]$, so that oscillations completely out of phase with one another will have a phase difference of 0.5. The phase-delay spectrum was obtained by averaging cross-spectra over the frequency range 4-8 Hz, corresponding roughly to the full width at half maximum of the QPO peak.

There is a clear jump in the phase-delay spectrum. X-ray intensity fluctuations in all the energy channels above ~ 3.5 keV are in phase with one another, but out of phase with fluctuations in the two lowest energy channels. The phase difference between channels 1-2, covering 1.2-3.5 keV, and channels 5-10, covering 5.8-18.4 keV, is ~ 0.42 , or 150° .

One procedure to measure the phase jump would be to fit the observed phase-delay spectrum using a function that is asymptotically flat at high and low values, and quickly turns over. Alternatively, one could average the phase delay spectrum over the high energy channels and over the low energy channels and measure the difference. Our χ^2 procedure used to determine the phase-delay spectrum introduces non-zero covariances between the points in Fig. 1. The goodness of fit criterion used in fitting, or the weighting for averaging, would thus have to incorporate the covariances. A simpler alternative is to measure the

phase delay between the two lowest energy channels (1.2-3.5 keV) and the six highest energy channels (5.8-18.4 keV) using a standard cross spectrum, and average over the same range of Fourier frequencies (4-8 Hz) used to determine the phase-delay spectrum. Because the phase differences between the two lowest energy channels, and among the six highest energy channels are small, this is reasonable and we followed this approach. The phase difference we find in this way is $\delta\phi = 0.42 \pm 0.03$ (1σ), or $151^\circ \pm 11^\circ$. The phase delay is not exactly 180° , but 2.7σ different from this value. The oscillations at high energies lag those at low energies by 151° , or 70 milliseconds.

As discussed in the previous section, instrumental deadtime induces an anticorrelation between intensity fluctuations in different energy channels. Because the observed time delay is near 180° , we checked that we were not looking at an instrumental artifact. Simple fixed deadtime per event, such as is present in *Ginga*, affects only the real part of the cross spectrum. The 2.7σ positive imaginary part we observed is therefore not instrumental. We tested all three of the techniques discussed in Sect. 3.2 to correct for instrumental deadtime. We found that phase differences measured using method 3 agreed well with those determined by method 2. We found discrepancies when we attempted to correct the raw cross spectra using method 1, subtracting the measured average cross spectrum at high frequencies. Lewin et al. found that there is considerable power at the highest accessible frequencies. Thus, there is no frequency range available in which Poisson fluctuations dominate the cross spectrum, as required for method 1 to work. We strongly recommend calculating cross spectra with data converted to counts per live time, provided the deadtime process is well understood, because it is simple to implement, and effectively eliminates both types of cross talk. See, however, Sect. 3.2 for limitations on applicability. Results reported here were all derived using method 3.

Because we defined the lower normal branch differently than Lewin et al. (1992), we remeasured the rms-amplitude spectrum of the lower normal branch. We also wanted to check that QPO fractional rms amplitudes measured with data converted to counts per live time were consistent with amplitudes obtained by applying the corrections described in Lewin et al. (1992) to fractional rms amplitudes determined from fits to power spectra of raw data. As a fit function we employed a power law to describe the red noise and a Lorentzian to describe the QPO peak.

We first fitted the total power spectrum of the lower normal branch data and then fitted the power spectra in the separate energy bands while fixing the value of the QPO centroid frequency, ν_{QPO} , and full width at half maximum, Γ , at the values found from the total data. We fixed the power law index at 0.4 as found by Lewin et al.. The power level induced by counting statistics, the so-called Poisson noise level, we calculated from the theoretical distribution of counts per bin as modified by instrumental deadtime. We obtained best fit values of $\nu_{QPO} = 5.9 \pm 0.2$ Hz and $\Gamma = 4.3 \pm 0.3$ Hz, with $\chi^2 = 30.1$ for 22 degrees of freedom. We found a local minimum in χ^2 at $\Gamma = 6.4$ Hz, the value reported in Lewin et al., but with a larger value of χ^2 . To test

the sensitivity of the rms-amplitude spectrum to Γ , we fitted the power spectra with both $\Gamma = 4.3$ Hz and with $\Gamma = 6.4$ Hz, and found only small differences in fractional rms amplitude. In all cases, values obtained using data converted to counts per live time agree with values obtained by transforming raw data then correcting the measured amplitudes (van der Klis 1989a; Lewin et al. 1992), and are the same, to well within measurement uncertainties, as those reported in Lewin et al.. We found, as did Lewin et al., that it was necessary to combine the two lowest energy channels (covering 1.2-3.5 keV) in order to detect the QPO. The count rate in the lowest energy channel is 400 counts per second, a factor of 5 lower than in the next several channels. We do not detect QPO in that channel, with a 1σ upper limit to the fractional rms amplitude of the QPO of ~ 0.01 . The rms amplitude of the QPO in the two lowest channels combined is 0.005 ± 0.002 . Thus, we see no evidence for a minimum in the QPO rms amplitude spectrum at 3.5 keV, but we cannot exclude the existence of such a minimum, consistent with the results of Lewin et al. (1992).

5. Discussion

On the lower normal branch, where GX 5-1 shows pronounced 6 Hz QPO, the phase-delay spectrum shows a clear jump in the phase of 4-8 Hz X-ray intensity variations below and above 3.5 keV (Fig. 1). We calculated the phase-delay spectrum that would result from an incident photon spectrum that rocks about a pivot energy of 3.5 keV and found that the observed jump is statistically consistent with a perfectly sharp jump at 3.5 keV, but that the observed phase difference, 151° , is inconsistent with the 180° shift predicted by a rocking spectrum. The rocking spectrum model also predicts a minimum in rms-amplitude at the jump energy. Indeed, a minimum is seen in the rms-amplitude spectrum of normal-branch QPO in Cyg X-2 at the same energy as the turnover in the phase-delay spectrum, consistent with a rocking spectrum. We see no such minimum in GX 5-1, but we cannot exclude that a minimum as predicted by the rocking spectrum model is present. Dotani (1988) sees weak evidence for a minimum in QPO fractional rms amplitude at 3.5 keV in normal branch data obtained during a 1988 observation of GX 5-1.

A number of models have been proposed to explain normal-branch QPO. The radiation-hydrodynamics model (Lamb 1989, 1991; Fortner & Lamb 1989) is the most detailed. In this model, hot material from the inner edge of the accretion disk falls radially onto the neutron star, comptonizing low-energy ($E \sim 1$ keV) photons produced in a small magnetosphere. When the mass accretion rate approaches the Eddington rate, global oscillatory modes in the inflow cause the x-ray spectrum to vary quasi-periodically at the freefall time, as modified by radiation pressure, producing normal-branch QPO. Others have proposed that the inner accretion disk puffs up at high mass accretion rate so that the inner disk resembles a torus with the neutron star at its center (van der Klis et al. 1987). Alpar et al. (1992) point out that the Kepler rotation period in the inner disk is affected by radiation pressure in the same way as the freefall time. Oscillations in density and optical depth in the

torus have the same characteristic time scale as oscillations in a radial flow, and could be the source of normal-branch QPO. As in the radiation-hydrodynamics model, hot material from the inner disk is responsible for Comptonization. In either case, if the QPO arise from quasi-periodic changes in the optical depth of the Comptonizing material, a $\sim 180^\circ$ jump is expected in the phase of the oscillations. The jump energy, E_j , is determined by the electron temperature, T_e , of the Comptonizing plasma (Fortner et al. 1989; Lamb 1989).

The energy of the jump in GX 5-1 is different from E_j observed in normal-branch data from Cyg X-2 (Mitsuda & Dotani 1989). It is ~ 3.5 keV in GX 5-1, and ~ 6 keV in Cyg X-2, yet the systems are in other ways twins. The frequency, width and amplitude of normal-branch QPO are nearly identical (Mitsuda & Dotani 1988; Lewin et al. 1993), as are magnitude and sign of the phase-delay. Both are in the same subcategory of Z-source based on the shape of their color-color diagrams, their power-spectral behavior, and the secular motion of their “Z” pattern (Hasinger & van der Klis 1989; Penninx et al. 1991; Kuulkers et al. 1994). These similarities strongly suggest the same physical mechanism is responsible for the QPO in the two systems, and that a subset, at least, of the physical parameters are nearly equal.

As a Z source moves down the normal branch toward the flaring branch its spectrum softens. This softening is clear in both color-color and hardness-intensity diagrams. Psaltis, Lamb & Miller (1995) have found that the temperature of the radial flow decreases along the normal branch, and Schulz & Wijers (1993) find that T_e decreases along the normal branch toward the flaring branch from fitting a Comptonization model to the energy spectra of Z sources. We thus propose that E_j is higher in Cyg X-2 because it was observed at a higher (harder) position on the normal branch than GX 5-1. In order to compute phase delays, Mitsuda & Dotani (1989) combined all high time resolution data containing normal-branch QPO from their 1987 Ginga observation of Cyg X-2. The data showing strong QPO were all on the middle to upper (hard) part of the normal branch. In contrast, we see QPO only on the lower normal branch in GX 5-1.

On the basis of their flaring behavior, noise characteristics and optical properties, it has been suggested that the Z sources GX 5-1, Cyg X-2, and GX 340+0 are viewed at high inclination (Kuulkers et al. 1994; Cowley et al. 1979; Bonnet-Bidaud & van der Klis 1982; Vrtilik et al. 1986). Of the 3, GX 5-1 is thought to have the highest inclination (Kuulkers et al. 1994). As a result, when the inner accretion disk flares up, the neutron star and the radial flow are obscured from sight. This will occur at a lower mass accretion rate in GX 5-1 than in Cyg X-2. Normal branch QPO can only be observed if the accretion rate is high enough to excite oscillatory modes. It is possible that when the QPO are first excited, they are obscured in GX 5-1, but visible in Cyg X-2. In the radiation hydrodynamics model, as the accretion rate increases, the outer boundary of the radial infall moves out. When the infall region becomes visible, QPO are observed. This will only occur if the infall region grows faster with mass accretion rate than the vertical scale of the inner disk.

This picture favors a central origin for the QPO oscillations over a torus. It also leads to the prediction that E_j will decrease with position on the Z. Finally, we predict that it will be possible to observe E_j at energies above 6 keV in the remaining Z sources, which are thought to be viewed at lower inclination. Of course, E_j will still depend upon position in Z in these sources. The nondetection of time delays in Sco X-1 (Dieters et al., in preparation), possibly due to E_j being even less in that observation than in ours of GX 5-1, may be due to a location of this source further down the normal branch during their observation.

Acknowledgements. WHGL acknowledges support from the National Aeronautics and Space Administration under Grant NAG8-674. This work was supported in part by the Netherlands Organization for Scientific Research (NWO) under grant PGS 78-277.

References

- Dotani, T. 1988, PhD Thesis, University of Tokyo (ISAS Research Note 184).
- Fortner, B., Lamb, F. K., & Miller, G. S. 1989, *Nature*, 342, 775.
- Hasinger, G., and van der Klis, M. 1989, *A&A*, 225, 79.
- Hertz, P. and Grindlay, J. E. 1984, *ApJ*, 282, 118.
- Lamb, F. K. 1989, in Proc. 23rd ESLAB Symposium on Two Topics in X-ray Astronomy, ed. J. Hunt & B. Battrick, ESA SP-296, 215.
- Lamb, F. K. 1991, in *Neutron Stars: Theory and Observation*, ed. J. Ventura & D. Pines (Dordrecht: Kluwer Academic Publishers), 445.
- Lewin, W., van Paradijs, J., and van der Klis, M., 1988, *Space Sci. Rev.*, 46, 273.
- Lewin, W. H. G., Lubin, L. M., Tan, J., van der Klis, M., van Paradijs, J., Penninx, W., Dotani, T., & Mitsuda, K. 1992, *MNRAS*, 256, 545.
- Makino, F., and the Ginga ASTRO-C Team, 1987, *Astrophys. Letters mmun.*, 25, 223.
- Miller, G. S. & Lamb, F. K. 1992, *ApJ*, 388, 541.
- Mitsuda, K., & Dotani, T. 1989, *PASJ*, 41, 557.
- Norris, J. P., Hertz, P., Wood, K. S., Michelson, P. F., Vaughan, B. A., Mitsuda, K., and Dotani, T. 1990, *ApJ*, 361, 514.
- Turner, M. J. L., Thomas, H. D., Patchett, B. E., Reading, D. H., Makishima, K., Ohashi, T., Dotani, T., Hayashida, K., Inoue, H., Kondo, H., Koyama, K., Mitsuda, K., Ogawara, Y., Takano, S., Awaki, H., Tawara, Y., and Nakamura, N. 1989, *Pub. Astr. Soc. Japan*, 41, 345.
- van der Klis, M., Jansen, F., van Paradijs, J., Lewin, W. H. G., van Heuvel, E. P. J., Trumper, J., and Sztajno, M. 1985, *Nature*, 316, 225.
- van der Klis, M. 1989a, in *Timing Neutron Stars*, ed. H. Ogleman & E. P. J. van den Heuvel (Dordrecht: Kluwer Academic Publishers), 27.
- van der Klis, M. 1989b, *ARA&A*, 27, 517.
- Van der Klis, M., Hasinger, G., Stella, L., Langmeier, A., van Paradijs, J., and Lewin, W. H. G., 1987, *ApJL*, 319, L13.
- Vaughan, B., van der Klis, M., Lewin, W. H. G., Wijers, R. A. M. J., van Paradijs, J., Dotani, T. & Mitsuda, K. 1994, *ApJ*, 421, 738.